Evolutionary Models of Convergent Margins : Origin of Their Diversity

Chapter 9

Oki-Dozen Dike Swarm: Effect of the Regional Stress Field on Volcano-Tectonic Orientations

Daisuke Miura, Kiyoshi Toshida, Ken-ichi Arai,
Takeshi Wachi and Yutaka Wada

Additional information is available at the end of the chapter

http://dx.doi.org/10.5772/67612

Abstract

This article presents new field, geochronological, and geochemical data for the Late Miocene Oki-dozen dike swarm (ODS), southwest Japan. This swarm is part of a volcanic suite comprising mafic and silicic dikes, sills, and pyroclastic cones from which we obtained structural measurements at a various genetic orders and scales. The mafic magmas generated three dike swarms with dikes oriented to NW-SE, N-S, and NE-SW. In comparison, the silicic intrusions do not have a preferred orientation but instead appear to radiate from the center of the volcanic suite. Comparison of the maximum thickness of 37 dikes with SiO_2 content (wt%) yielded a critical thickness (T_{cr}) value of $T_{cr} = 0.2 \times (SiO_2 - 40)$. These data indicate that the orientations of dikes were controlled by the magnitude of dike tip pressure and magma overpressure, both of which positively correlate with SiO_2 concentrations. The silicic units yield estimated pressures (up to 15–60 MPa) that are large enough to have counteracted the regional stress field, whereas the mafic dike swarm only yielded lower pressures. This result suggests that comparative analysis at a range of scales is essential for the accurate determination on the tectonic stress field by igneous rocks.

Keywords: dike, sill, mafic magma, silicic magma, stress field, volcanology

1. Introduction

Geological research into the formation of subvolcanic structures can provide insights into the long-term processes that contribute to magma plumbing and migration. One

example of these processes is the formation of a dike swarm, where single dike formation involves a physical process in the form of crack opening [1, 2]. The ambient stress field during dike intrusion can be modeled as a mode 1 open crack that is associated with liquid magma injection [3]. This process occurs over timescales of hours to months, meaning that any physical contrasts in properties between the magma and the host rock are key controls on dike emplacement. The analysis of deformation structures within dike interiors can provide information on dike propagation processes prior to eruption [4–6]. However, dike swarms form as a result of the repeated injection of blade-like magma bodies into the crustal subsurface, a process that can take several ten of years, a thousand years, or more. Subvolcanic structures such as dike swarms form as a result of numerous competing geological factors, which include the following: the behavior of magma in stiff host rock(s); the physical properties of magma; local, regional, and tectonic stress fields; and the structure of the host rocks.

Changes in magma density and/or viscosity can provide insights into the behavior of magmas in deep-seated blade-like conduits. The rheological properties of magma usually govern the eruption rate, the kinetics of crystal and bubble formation, and the flow of lava on the Earth's surface [7]. Magmas can have a wide range of viscosities [8–11] that in turn lead to diverse eruption styles, structures, and evolution of eruptive episodes. The viscosity of a molten magma varies between 10^2 and 10^8 Pa s [12], and bulk viscosity dramatically increases with decreasing magma temperature and increasing crystal abundance. For example, a bulk magma with a crystal fraction of >0.6 may not be eruptible [13], and this limit of "eruptibility" is a critical threshold for the emplacement of viscous magmas into a crack-type conduit [11, 14].

The Oki-dozen volcanic complex (OVC) is a volcanic suite located 300 km from the present-day subduction trench in SW Japan (**Figure 1**) [15–21]. The complex contains numerous volcanic edifices that define the interior of the complex, including an outer-flank basaltic volcano with lava flows, pyroclastic cones, dikes, and laccolithic sills. These intrusive bodies are here termed the Oki-dozen dike swarm (ODS). The ODS includes ≥200 numbers of outcropping dikes and sills that allow the multiscale measurement of structural elements, in turn providing insights into the genetic relationships between the sills and dikes of the ODS.

Our new data from the ODS indicate that the propagation direction of dikes was controlled by pressure change in the dike interior and the state of the regional stress field. The presence of magma overpressure associated with magma density and magma chamber depth results in a distinctive pattern of dike orientation compared with the surrounding regional stress field (σ_3). This means that the development of a regional-scale dike swarm must involve the repetition of similar processes to produce dikes with a preferred orientation. This in turn indicates that a comparative analysis of the stress field at different scales is needed to infer the tectonic stress orientation in the volcanic rocks.

http://dx.doi.org/10.5772/67612

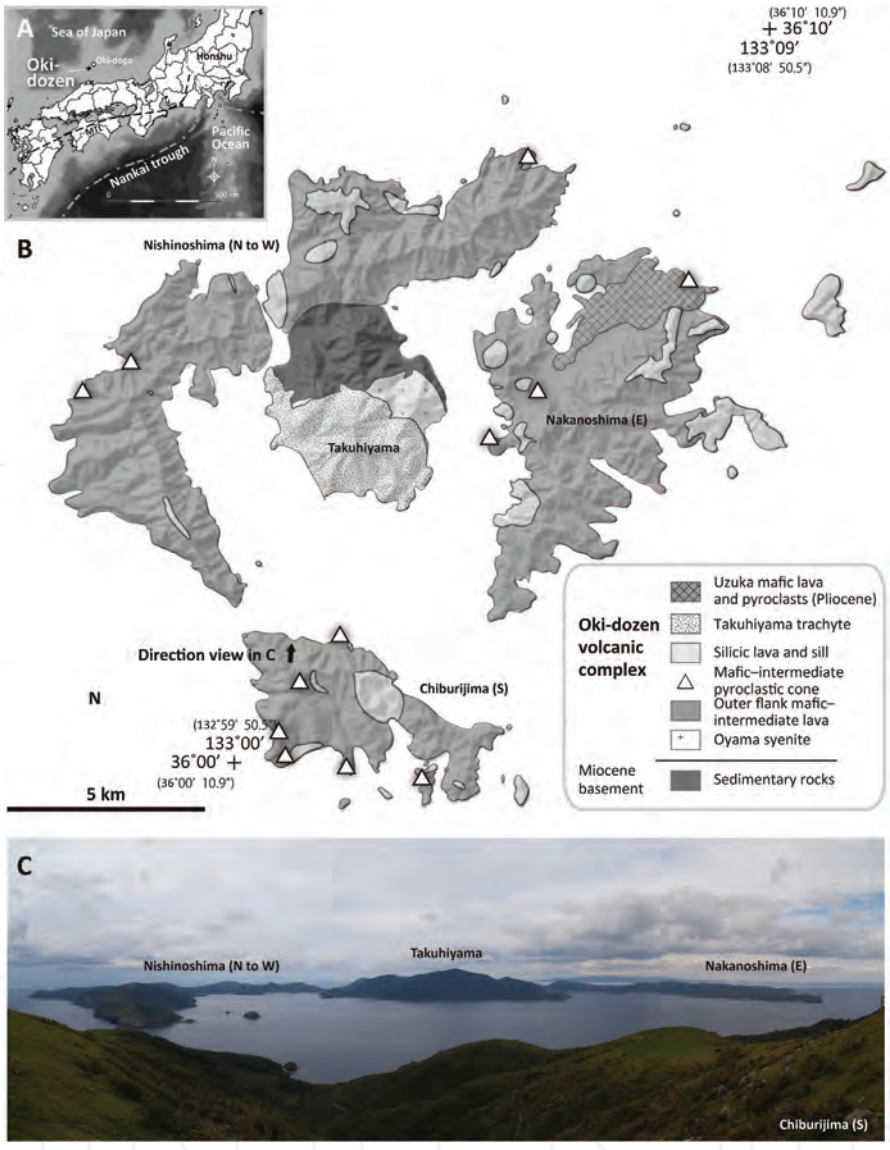

Figure 1. Maps showing the location (A) and geology (B) of the Oki-dozen volcanic complex (OVC) in southwest Japan (simplified after Refs. [16, 19]), and a panoramic view (C) of the topography of this region. The three main islands within the OVC are dominated by voluminous mafic lavas and laccolithic silicic intrusions that are associated with minor amounts of syenite and trachyte ash-flow tuff. Miocene sedimentary rocks, the Oyama syenite, and the Takuhiyama trachyte ash-flow tuff all crop out within the central OVC, suggesting this area is underlain by a fossil magma chamber. The open triangle in (B) indicates the location of a pyroclastic cone that represents a conduit for both mafic and silicic magma systems, as well as an area that concentrated mafic and silicic magma conduits.

2. General geology of the Oki-dozen volcanic complex

2.1. Geologic setting

The Oki-dozen islands of southwest Japan consist of the latest Miocene dissected OVC (**Figure 1**) [15–21], which is located in the southern Sea of Japan, ~50 km off the north coast of Shimane Peninsula, 15 km southwest of Oki-dogo island. The Oki-dozen islands comprise three main islands: Nishinoshima, Chiburijima, and Nakanoshima (**Figures 1** and **2**). These islands form part of the Oki-Shimane plateau within the Sea of Japan [22], and parts of these islands have been awarded UNESCO Global Geopark status as a result of the large number of excellent exposures of volcanic deposits [15].

The interior of the complex consists of the ODS, which comprises a suite of numerous volcanic edifices that include an outer-flank basaltic volcano, lava flows, pyroclastic cones, dikes,

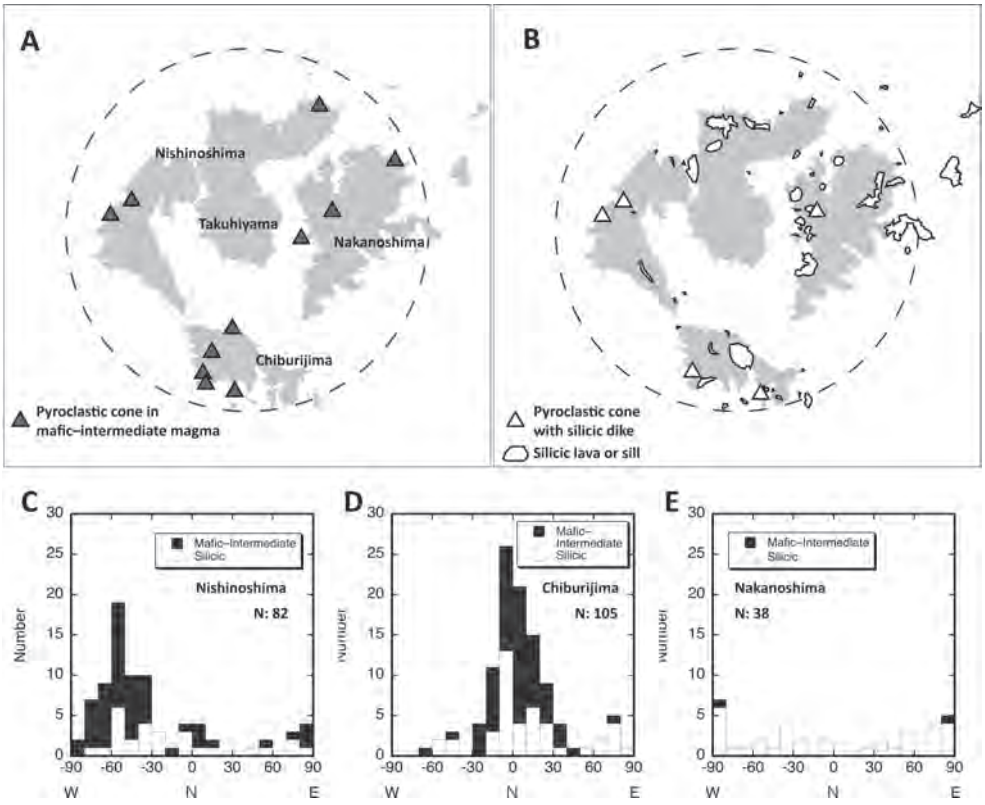

Figure 2. Overview map showing the location of magma source vents for the mafic (A) and silicic (B) magmas within the interior of the OVC, and histograms (D–F) showing the preferred orientation of the Oki-dozen dike swarm (ODS) (after Ref. [16]). These maps and diagrams indicate that the mafic magmatism in this area has NW-SE and N-S preferential orientations on Nishinoshima (D) and Chiburijima (E) islands, whereas the silicic magmatism in this area defines a radial pattern.

http://dx.doi.org/10.5772/67612

and laccolithic sills. The multiple mafic and silicic dike swarms of the ODS are located within the alkaline OVC and represent an ideal area for determining the processes involved in dike propagation and emplacement for the following reasons. (1) The ODS formed rapidly (within a million years), as evidenced by precise K-Ar ages of 5.9–5.5 Ma for the majority of the stratocone lavas and associated dikes and sills in this region [16]. In addition (2), the OVC is a volcanic suite that is located ~300 km from the present-day subduction trench in SW Japan, and (3) the coeval magmatism in this region formed ≥200 single, composite, and multiple dikes, pyroclastic cones, and sills [15–18]. Finally, (4) the ODS has a broad range of magma compositions with SiO_2 concentrations of 44–69 wt% [15–18].

This study presents multiscale structural data for a couple of hundred dike and sill outcrops, providing insights into the relationships between structures, stress, and dike and sill emplacement. The mafic trachybasalt and trachyandesite magmatism formed three swarms of parallel dikes oriented to NW-SE, N-S, and NE-SW. In contrast, the silicic trachytic intrusions show no preferential orientations but instead radiate from the central OVC. These differences suggest that the silicic magmas were emplaced into a volcano-related regional stress field in which the horizontal stress was similar in all directions.

2.2. Ages

Many radiometric dates have been reported for the OVC. Zircon U-Pb ages of 6.3–6 and 6.2–5.7 Ma have been reported for the subplutonic Oyama syenite and the Takuhiyama trachyte, respectively [15]; an anomalously old age of 7.4 Ma has been obtained for the Oyama syenite [18, 19]. Precise K-Ar dating of the majority of the stratocone lavas and associated ODS dikes and sills yields ages of 5.9–5.5 Ma (**Figure 3**) [16]. Another anomalously young age of ca. 2.8 Ma has been reported for a scoria cone and lava flows of the Uzuka basalt in the Nakanoshima area. These age data suggest that ODS was rapidly emplaced over <1 Myr, as evidenced by the precise K-Ar dates of 5.9–5.5 Ma outlined above [16].

The genetic order in a series of alkaline magmas was temporally and spatially coeval (**Figure 4**). For example, in **Figure 4A**, the silicic dike/sill has intruded into the mafic scoria cone, whereas the mafic trachyandesite dike has later intruded along the marginal part of the silicic dike at

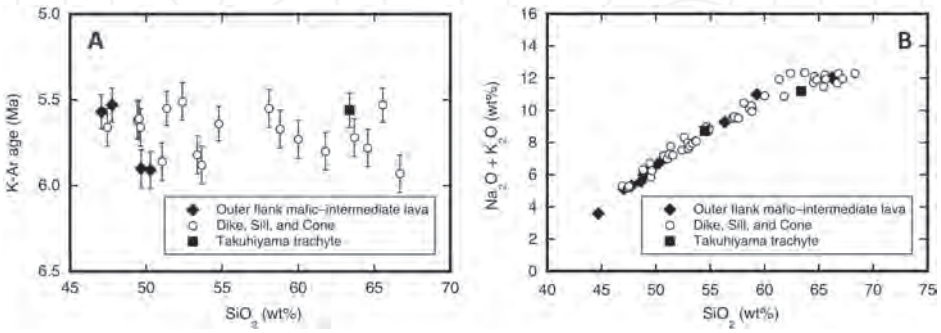

Figure 3. K-Ar age vs. SiO_2 concentration (A) and total alkali vs. silica SiO_2 – $Na_2O + K_2O$ (B) (modified after Ref. [16]) diagrams for the samples analyzed during this study.

center. This finding suggests that an arbitrary stress field, which was temporally coeval with Late Miocene tectonics, must have resulted in the variation for preferred orientations of the ODS.

2.3. Stress field

The ODS is thought to have been emplaced into a neutral or weak transpressional stress regime, primarily as the silicic intrusions of the ODS have a range of orientations (**Figure 2**) [16]. The mafic dikes that originate from the center of the OVC have at least NW-SE and N-S orientations, and additionally dikes oriented to NE-SW are presumed, although only poorly exposed sections of dike are present within the Nakanoshima area. The eastern OVC contains scoria pyroclastic cones that have a NE-SW orientation (**Figure 2A**), suggesting that the mafic conduits in this area are aligned in three different directions. These orientations may directly reflect the nature of the tectonic stress field over an area of >100 km wide [20, 23]. This contrasts with research into back-arc opening and counter compression regime in SW Japan, which identified N-S compression and related folding of Late Miocene units [22]. The presence of diverse dike orientations within the ODS is inconsistent with this interpretation of the regional tectonic

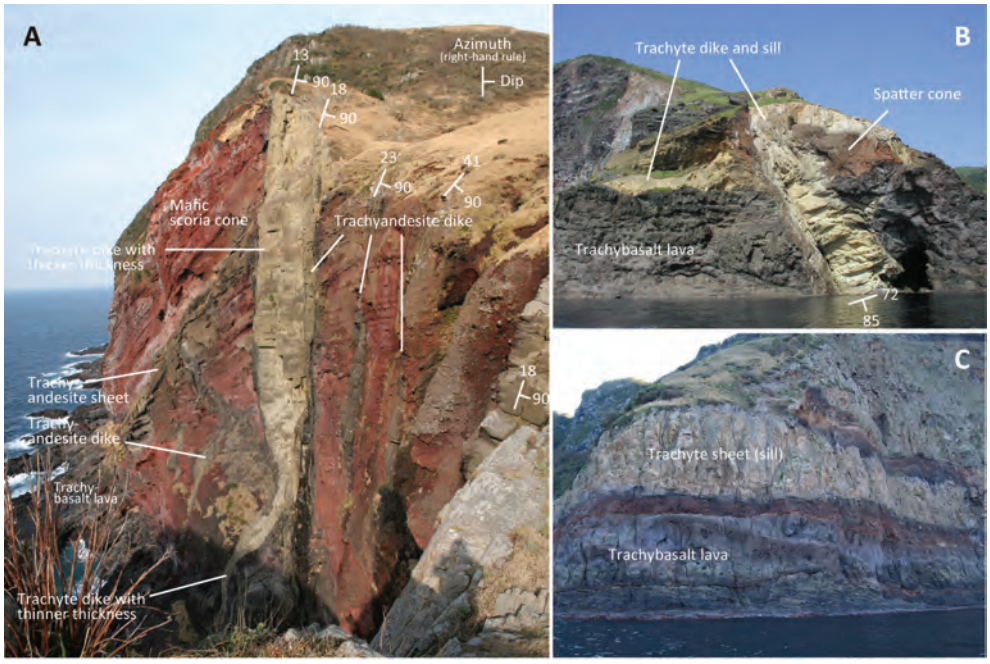

Figure 4. Examples of the relationships between pyroclastic cones and stratified lavas within the ODS. (A) A red-colored (a darker grey in greyscale) mafic scoria cone that forms a famous natural monument called Chibu-no-Sekiheki. The cone is cross-cut by trachyandesite and trachyte dikes and inclined sheets, with the thickness of a trachyte dike clearly varying as a result of host-rock stiffness, where the dike has a thickness of 4 m within stiff lavas and 17 m within soft pyroclastic ejecta [30]. (B) A spatter-rich pyroclastic cone called Byobu-iwa, where a yellow-colored (a pale in greyscale) trachytic dike-sill cross-cuts the cone. The images shown in (A) and (B) indicate that different magma conduits coalesced during the formation of the OVC. (C) A trachytic laccolith sill emplaced into stratified trachybasalt lava flows.

http://dx.doi.org/10.5772/67612

stress field. The magnitude and longevity of the stress field associated with a magmatic intrusion depend on the diversity in length, or area of distribution, of stress indicators such as dikes. Magma-generated stress fields are commonly short-lived [24]. In fact the ODS case, the massive syenite body aged in 6–7 Ma, acting as a core of volcanic suite, could have modified the regional stress regime from tectonics origin. This is a sense coincident with the modeling of geochemical study [15]. The model suggested that the basaltic magma injections were arrested by the syenite core in the center, whereas it could be readily reached to the outer region surfaces. Therefore, it is unclear whether the stress indicator of magma bodies in the study area reflects the size and long-term state of the tectonic stress field.

This article uses the following terminology for the size of the stress field at different scales: local stress field: 10^{-2} to 10^{3} m^2 (i.e., equivalent to a square with sides of 0.1–31.6 m in length); regional stress field: 10^{4} to 10^{7} m^2 (100–3162 m); and tectonic stress field: 10^{8} to 10^{10} m^2 (10–100 km).

2.4. Dissection depth at ODS

The ODS has undergone shallow dissection, with the center of the OVC containing outcropping sedimentary basement that appears to be at present-day sea level. The volcanic edifices in the study area and the sedimentary basement of the Ichibu and Shimazushima formations have not undergone any significant tilting [18]. In addition, the presence of numerous pyroclastic cones provides evidence of the paleosurface during eruption. The topography of the study area is the highest at Nishinoshima (451 m above sea level (asl)), with other peaks at Chiburijima (325 m asl) and Nakanoshima (256 m asl). These topographic highs mark the approximate land-surface level at the time of magmatic activity. Borehole data from Nakanoshima show a basal breccia unit within the OVC at a depth of >345 m below sea level [21]. This means that the depth of these units (D) is estimated to be 250–600 m from the original surface, yielding a lithostatic pressure of 6.9×10^{6} to 1.6×10^{7} Pa for a host rock density of 2800 kg m^{-3}.

2.5. Analytical methods

We measured the orientation, thickness, offset, and overlap between dike segments and collected samples from the ODS during this study. Sample preparation and analysis were undertaken at the Central Research Institute of Electric Power Industry (CRIEPI), Abiko, Japan, with thin sections of representative samples prepared for petrographic analysis. Modal phenocryst proportions were determined using an automated point counter and ≥2500 counts per thin section. Whole-rock major element concentrations on 54 lava flow, dike, and sill samples of >2 cm in diameter (i.e., excluding fine-grained layers) were determined using X-ray fluorescence (XRF) spectrometry employing a Shimazu XRF-1500 spectrometer with a rhodium tube [25]. Prior to analysis, washed and dried rock samples were powdered using an agate mill before being fused to form glass disks for analysis. These XRF analyses were calibrated using Geological Survey of Japan JR-3, JB-2, JGb-2, JH-1, JSy-1, and JSd-2 standards. Representative geochemical data of samples from the ODS are given in **Figure 3**.

3. Characteristics of the Oki-dozen dikes

3.1. Geochemistry

Volcanic rocks of the Late Miocene OVC have a broad range of alkaline compositions and contain 44–69 wt% SiO_2 [15, 16, 18]. The ODS can be divided into three types of alkaline rocks on the basis of a total alkali-silica diagram (**Figure 3**) [26], namely trachybasalt, trachyandesite, and trachyte groups. The trachybasaltic and trachyandesitic magmas formed piles of lava flows, spatter-rich pyroclastic cones and maars, pyroclastic surges, and ballistic ejecta, all of which were associated with strombolian and phreatomagmatic eruptions. The lavas and pyroclastic deposits are crosscut by numerous mafic, intermediate, and silicic intrusions, the majority of which are subvertical dikes although some trachytic rocks occur as subhorizontal or inclined laccolithic sills. The ODS also contains a trachytic ash-flow tuff and a subplutonic syenite body, both of which crop out within a small caldera in the Takuhiyama area of the central OVC [21].

3.2. Phenocryst abundances

Phenocrysts make up <26 vol% of the samples from the study area (**Figure 5**), suggesting that the crystal volume fraction of these magmas had a negligible effect on viscosity [13, 27]. This in turn indicates that the viscosity of the ODS magmas was controlled by SiO_2 content rather than crystal abundance.

3.3. Viscosity

The viscosity of mafic-intermediate magmas (i.e., magmas containing 44.8–56.3 wt% SiO_2) within the ODS has been previously measured and estimated [28, 29], yielding viscosities of 1.90–3.00 log poise at 1300–1122°C, corresponding to 0.90–2.00 log Pa s. Assuming these magmas were Newtonian fluids, they are inferred to have had low viscosity and low internal pressure (P_{om}). This characteristic generally results in thinner dikes as a result of the low magma overpressure against the ambient stress σ_3 at the dike wall.

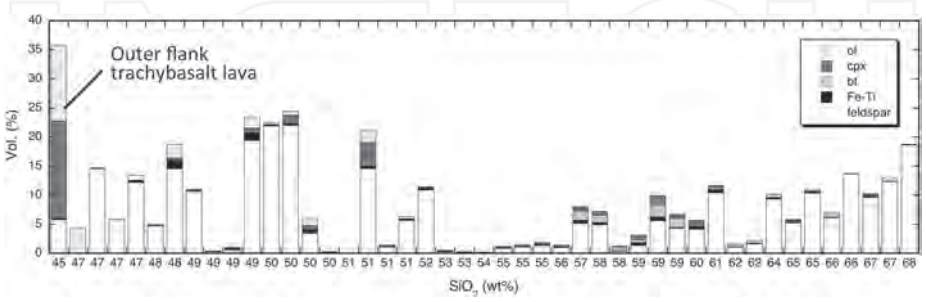

Figure 5. Variations in phenocryst type and abundance with changing SiO_2 concentration within the ODS rocks (modified after Ref. [16]). Abbreviations: ol: olivine; cpx: clinopyroxene; bt: biotite; Fe-Ti: Fe-Ti oxide minerals; feldspar: plagioclase and/or potassium feldspar.

http://dx.doi.org/10.5772/67612

4. Field observations

Extensive field measurements were made of the dikes and pyroclastic cones within the ODS, including location, orientation, and thickness measurements on more than 200 dikes and sills, their offsets, and overlaps where possible. The thickness associations with whole-rock SiO_2 concentrations have been discussed at the end of this section. The locations of pyroclastic cone were mapped (**Figure 2**) and the emplacement order of the associated dikes and sills was determined using structural relationships.

4.1. Pyroclastic cones

Typical relationships within the ODS are exemplified by pyroclastic cones and stratified lavas. One of these relationships forms the famous Chibu-no-Sekiheki natural monument, a red-colored mafic scoria cone with an interior that is crosscut by later trachyandesite and trachyte dikes and inclined sheets (**Figure 4A**). The trachyte dikes shown in **Figure 4A** vary in thickness as a result of variations in host rock stiffness, where the dike emplaced into stiff lavas is 4 m thick but bulges to a thickness of 17 m within soft pyroclastic ejecta. This difference is similar to that between feeder and nonfeeder dikes [30], although the difference observed in the study area reflects changing host rock stiffness rather than any variations in the flow of magma. The thicker trachyte dike was most likely caused by soft deformation of the host ejecta, a process that might have arrested dike ascent near the surface. The spatter-rich Byobu-iwa pyroclastic cone also contains a yellow-colored trachyte dike that was emplaced into stiff trachybasalt lavas before forming a laccolithic sill within the softer pyroclastic ejecta (**Figure 4B**). On the other hand, the outer-flank trachybasalt unit has a lot of laccolithic sills intercalated into the stratified lavas (**Figure 4C**). Those relevant trachyte forms massive intrusive bodies within the outer-flank trachybasalt lavas and are widely distributed across the OVC. The magmatic feeder system for trachyte sills in this area is evident as inclined sheets or subvertical dikes near the sill shown in **Figure 4**, indicating that many conduits containing magmas of various compositions coalesced during the formation of the OVC, regardless of their orientation.

4.2. Ideal dike segment shapes

The shape of a dike segment is a function of the physical processes involved in the intrusion of a magma as well as the propagation of a dike through the surrounding host rocks. A couple of distinctively shaped trachybasaltic dikes in the study area provide examples of different ideal dike shapes (**Figure 6**). The simplest case is exemplified by a teardrop-shaped trachybasalt dike (**Figure 6A** and **C**) that formed dike head, body, and tail segments as a result of magma flow. The bulging head of the dike formed as a result of the concentration of stress caused by excess magma pressure, contrasting with the narrow body and tail of the dike. The magma within the dike flowed from right to left in **Figure 6**, with pale orange-colored pyroclastic material filling a cavity at the tip of the head of the dike. Another

example is given in **Figure 6B** and **D**, which shows a bifurcating trachybasalt dike that is adjacent to a teardrop-shaped dike. The bifurcating head of this dike splits into two orthogonal sections whereas the main body projects straight toward the narrow tail of the dike. All of these observations indicate the direction of dike propagation toward the next dike, with the magma in this image of **Figure 6B** and **D** flowing from right to left, as for the teardrop-shaped dike. The bifurcating dike itself has a dike fingertip that is continuous toward the tail of the next teardrop-shaped dike. The surrounding brecciated host rock consists of numerous clasts within matrix material formed by hydrofracturing as a result of the injection of hot magma.

4.3. Structural relationships between dike segments

Structural relationships at dike tips are an important control on the form of connections between dike segments, which are a fundamental part of dike propagation. Here, we describe well-exposed outcrops that reveal the nature of connections between trachybasalt, basaltic trachyandesite, and silicic trachyandesite dike segments.

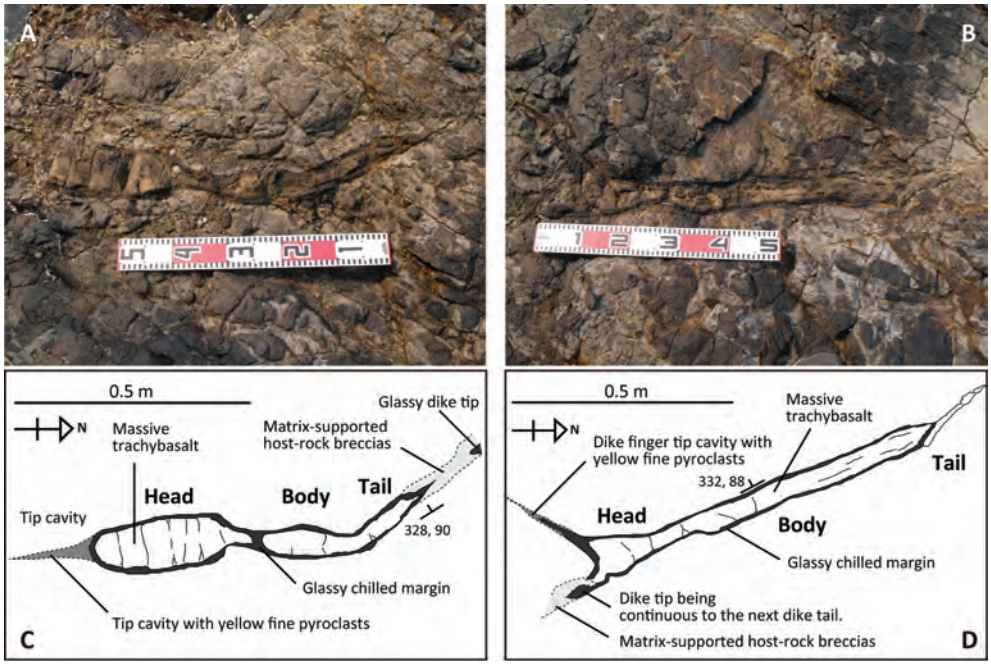

Figure 6. Examples of the ideal dike shape for trachybasalt magmas. (A) and (C) are a photograph and accompanying sketch showing a teardrop-shaped trachybasalt dike that provides evidence of a magma flow process that separated the magma into distinctive dike head, body, and tail sections. The bulging head shape formed as a result of the concentration of stress caused by excess magma pressure, with the inferred flow direction from right to left. Note the pale orange-colored (the grey in greyscale) pyroclastic material that fills the tip cavity space adjacent to the dike head. (B) and (D) are a photograph and accompanying sketch showing a bifurcating trachybasalt dike that flowed from right to left.

http://dx.doi.org/10.5772/67612

The coalescence of trachybasaltic dike segments in the Shiratori area of Chiburijima Island is shown in **Figure 7**, with these magmas recording the coalescence of two segments to form a hook- or pull-apart-shaped linking structure around the dike tips. The maximum thickness of the dike is 0.12 m, with offset and overlap distances between the two dike segments of 0.24 and 0.52 m, respectively. The trachybasalts in coalescing areas record the stepwise deformation of dike segments, with the host rock enclosed in these structures undergoing significant brecciation to form numerous large and small clasts and associated matrix material, most likely due to concentrated stress at the segment tip resulting in hydrofracturing. The host rock in this area is a stiff, massive, and uniform silicic laccolith, with soft-state deformation or brecciation possibly the result of episodic pressure increases caused by stress at the dike tip. This soft-state deformation caused the coalescence of the two dike segments.

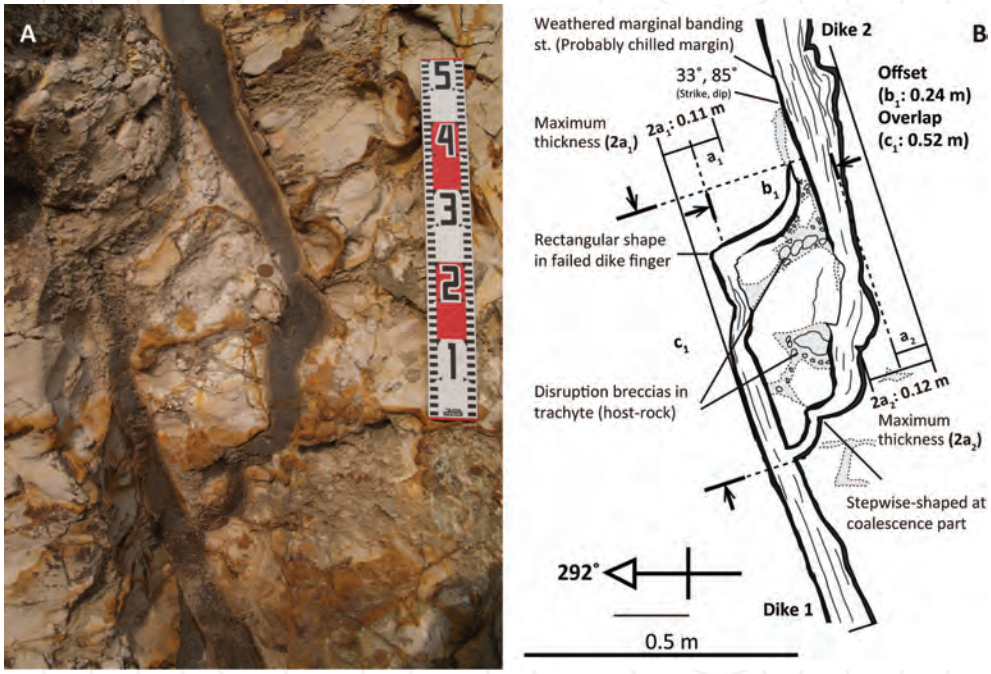

Figure 7. A hook-shaped structure linking dike segments within a trachybasalt. (A) Photograph and (B) explanatory sketch of the trachybasalt at Shiratori on Chiburi-jima island, where two segments of magma have coalesced to form a hook-shaped link (i.e., pull-apart shaped) structure around the dike tips. The host-rock enclosed in the structure is intensively brecciated and consists of numerous large and small clasts hosted by matrix material, all of which are thought to have formed by the concentration of stress at the segment tip and hydraulic fracturing (hydro-fracturing). The soft-state deformation around the dike tip induced the coalescence of the two segments. This dike is hosted by a stiff host-rock in the form of a less fractured trachyte intrusion. Abbreviations are as follows: a_1, a_2 = half maximum thickness, b_1 = offset length between dikes 1 and 2, c_1 = overlap length between dikes 1 and 2.

An offsetting of dike segments is also present within a basaltic trachyandesite dike in the study area (**Figure 8**), where an offset is present between two paper-knife-shaped dike tip segments. The hosting trachyte is brecciated and disrupted and has mingled with the dike magma, possibly related to the concentration of stress at the dike tip as well as hydrofracturing. The maximum thickness of this dike is 1.17 m, with offset and overlap distances between the two dike segments of 0.65 and 0.41 m, respectively. The glassy chilled margin of the dike contains a gently plunging lineation that suggests the magma in this area flowed horizontally.

Another offset relationship is visible within a silicic trachyandesite dike (**Figure 9**). This thick dike contains an offset in the form of a separate finger and formerly adjoined tail within two adjacent dike segments. The host rock is a stiff laccolith, and only weakly fractured trachybasalt lava and the dike have a maximum thickness of 1.33 m, with offset and overlap distances between the two tips of 1.96 and 1.18 m, respectively. These distances are larger

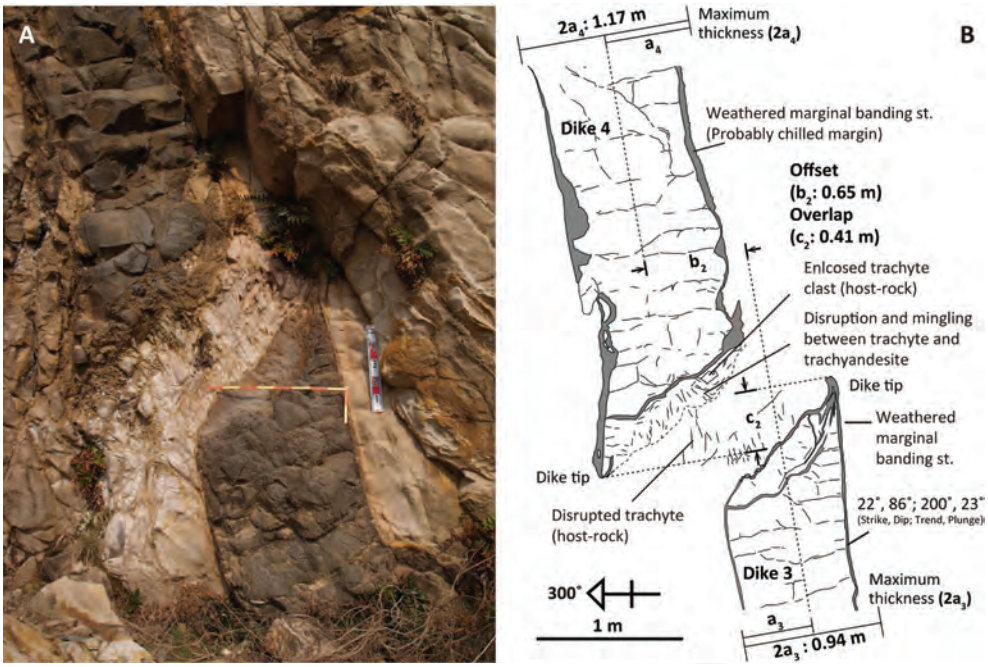

Figure 8. Basaltic trachyandesite dike segment offsets shown in a photograph (A) and accompanying explanatory sketch (B) of an outcrop at Shiratori on Chiburi-jima Island. Here, the magmas have been offset across two paper-knife-shaped tips located in different dike segments. The location contains brecciated, disrupted, and mingled trachyte host-rock and trachyandesite dike material. The surface of the glassy chilled margin in this area shows a gently plunging lineation, suggesting the magma in this area moved horizontally. Abbreviations are as follows: a_3, a_4 = half maximum thickness, b_2 = offset length between dikes 3 and 4, c_2 = overlap length between dikes 3 and 4.

http://dx.doi.org/10.5772/67612

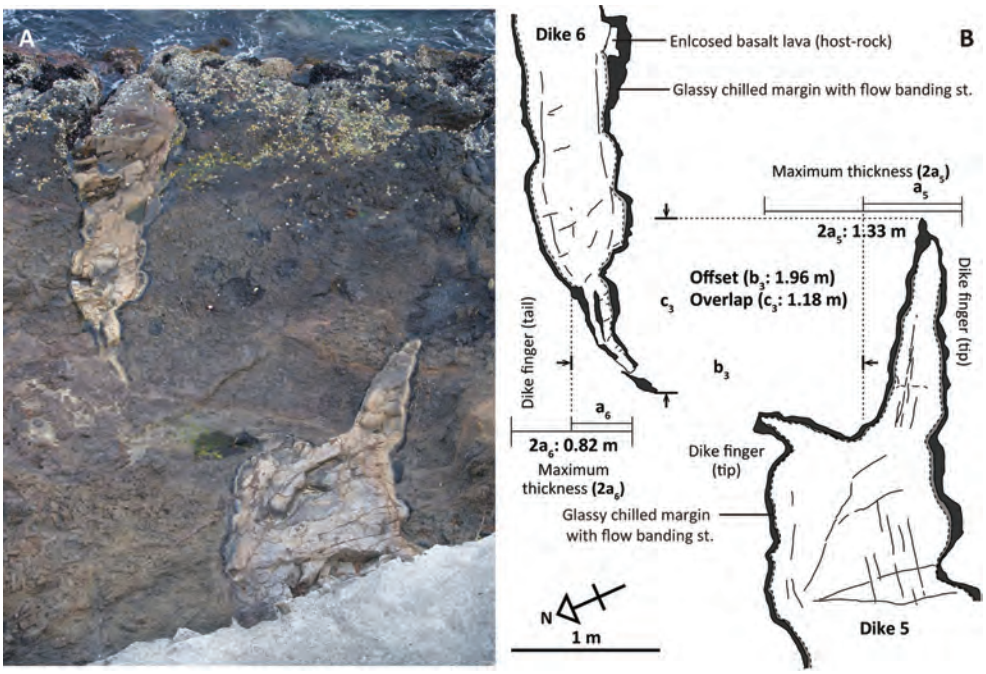

Figure 9. Offset relationship within silicic trachyandesite dike segments shown in a photograph (A) and an accompanying explanatory sketch (B) of an outcrop at Shimanehana on Nishinoshima Island. The thick trachyandesite dike is offset across the tips of the dikes visible in the figures. This dike was emplaced into a stiff and less-fractured trachybasalt lava. Abbreviations are as follows: a_5, a_6 = half of maximum thickness, b_3 = offset length between dikes 5 and 6, c_3 = overlap length between dikes 5 and 6.

than those determined for the trachybasalt and basaltic trachyandesite dikes discussed above (**Figures 7** and **8**), suggesting that the silicic trachyandesite dike experienced a greater concentration of stress than the other two dikes.

4.4. Relationship between critical dike thickness and SiO_2 concentration

The maximum thicknesses of the 37 ODS dikes were measured to determine a critical thickness value that correlates with SiO_2 concentration (**Figure 10A**). All of the dike sections measured during this study were hosted by stiff host lavas rather than soft pyroclastic ejecta. The relationship between dike thickness and SiO_2 concentrations yields a critical thickness (T_{cr}) threshold line that can be approximately modeled using $T_{cr} = 0.2 \times (SiO_2 - 40)$. This suggests that ODS dikes within stiff host rocks containing 75 and 80 wt% SiO_2 have maximum thicknesses of 7 and 8 m, respectively, contrasting with a trachytic dike emplaced into a pyroclastic cone that has a thickness of 17 m (**Figure 4**). The emplacement of this dike into the cone may have resulted in the soft-state deformation of the hosting ejecta, thereby arresting the ascent of the trachyte dike near the surface.

5. Discussion

5.1. Relationships among dike thickness, dike offset, and the overlap of dike segments

The ideal dike shape, dike tip relationships, dike thicknesses, dike offsets, and dike overlaps all provide information on the processes that operate during the propagation of a single dike in a given direction. A dike has a shape defined by its propagation direction and is subdivided into head, body, and tail segments (**Figure 6**). The dike head and tip bulge as a result of the concentration of stress (**Figure 6A** and **C**), a process that leads to dike propagation (**Figure 6B** and **D**). Offset and overlap structures form as a result of the magnitude of stress in a given part of the dike, where the concentrated stress is usually four times larger than the dike magma overpressure [2]. This means that the direction of dike propagation can change in areas with concentrated stress, although propagation outside of these areas is generally controlled by local and regional stress fields.

The relationship between offset (b) and overlap (c) yields a linear curve with a relatively gentle gradient $c = 0.7b$ (**Figure 10B**), whereas areas beyond $b = 0.6$ show a thickness ($2a$) to offset (b) relationship that yields a gentle curve, $a = 0.06b$. This reflects a difference in stress concentration between magma overpressure ($2a$) and the pressure at the dike tip (b), with the concentrated pressure at the dike tip drastically increasing with only a minor increase in magma overpressure.

5.2. Magma overpressures within mafic and silicic dikes

Dike magma overpressure can be estimated using fracture mechanics such as hydrofracturing [2], a process that is an important control on dike propagation and the formation of a dike

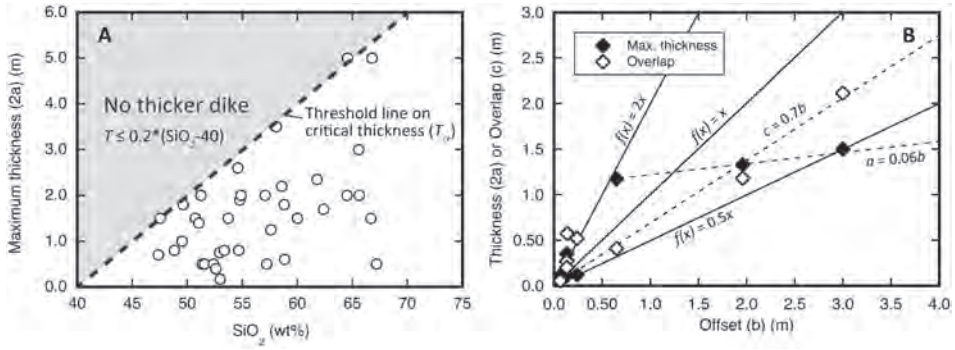

Figure 10. Relationship between SiO_2 concentration and maximum dike thickness (A), and offset distances to either overlap length or maximum dike thickness (B). (A) shows a threshold critical thickness line (T_{cr}) for the ODS magmas, where an empirical curve fit to T_{cr} is expressed as $T_{cr} = 0.2 \times (SiO_2 - 40)$. Assuming a thickness/length ratio of 1000 [2], we obtain dike lengths from 1.0×10^2 to 5.0×10^3 m, with these lengths relating to the regional stress field. (B) indicates that the offset (b) to overlap (c) relationship is roughly proportional to a linear curve fit where $c = 0.7b$, whereas the maximum thickness ($2a$) forms two distinct regions within a curved slope, with $0.6 \geq b > 0$ yielding a steep curve for $a \sim b$ and $b > 0.6$ yielding a gently sloping curve where $a \sim 0.06b$.

http://dx.doi.org/10.5772/67612

swarm. Generating a vertical hydrofracture from a source chamber at a given depth below the original surface involves the rupturing of a reservoir, with hydrofracturing initiating when the following condition is satisfied [2]:

$$p_l + p_e = \sigma_3 + T_0, \tag{1}$$

where p_l is lithostatic stress at the rupture site, $p_e = p_t - p_l$ is the difference between total fluid pressure p_t in the reservoir and the lithostatic stress p_l at the time of reservoir rupture, σ_3 is the minimum compressive principle stress, and T_0 is the local in situ tensile strength at the rupture site. The propagation of hydrofracturing leads to the magma overpressure p_o becoming

$$p_o = p_e + (\rho_r - \rho_m)\, gh + \sigma_d, \tag{2}$$

where p_e is the fluid excess pressure at the source, ρ_r is host rock density, ρ_m is magma density, g is acceleration due to gravity, h is the height of the given part of the hydrofracture, and σ_d is the differential stress at the level where the hydrofracture is being examined [2]. Hydrofracturing initiates when p_e becomes equal to the tensile strength T_0, which is usually T_0 = 0.5–6 MPa, yielding an average value of 3.25 MPa. Here, we simplify this problem by assuming that the stress difference σ_d is also equal to the tensile strength of the host rock, T_0. The host rock is the stiff trachybasalt lava, meaning that the average host rock density ρ_r and the average trachyte magma density ρ_m are 2800 and 2350 kg m^{-3}, respectively.

Clinopyroxene thermobarometric analysis of the OVC rocks yielded pressures of formation of 40–270 MPa for trachyte magma, a value that is consistent with the results of amphibole barometry for these units (<50 MPa) [15]. This means that the trachyte formed in a magma chamber at a pressure of 40–50 MPa, roughly equivalent to a depth of 1.5–2 km. The magma overpressure p_{os} of the trachyte magma can be given by

$$\begin{aligned} p_{os} &= 3.25 \times 10^6\ \text{Pa} + \left(2800\ \text{kg m}^{-3} - 2350\ \text{kg m}^{-3}\right) \times 9.8\ \text{m s}^{-2} \times \\ &\quad 2000\ \text{m} + 3.25 \times 10^6\ \text{Pa} = 1.53 \times 10^7\ \text{Pa} = 15.3\ \text{MPa}. \end{aligned} \tag{3}$$

Similarly, the magma overpressure of the trachybasalt magma p_{om} is given by

$$p_{om} = 6.5 \times 10^6\ \text{Pa} = 6.5\ \text{MPa}. \tag{4}$$

These results suggest that the trachybasalt magma reflects the ambient state of the regional stress, whereas the trachyte magma overpressure may override the regional stress field. We assume a dike length (along strike) to thickness ratio of 1000 [2] or 1500 [31], which are common values obtained from dike measurements worldwide [31]. A single dike has a length of several kilometers, a scale that is influenced by the regional stress field. The presence of regional horizontal differential stress ($\sigma_{H\max} - \sigma_{H\min}$) at a shallow level may cause the trachybasalt dike to propagate with a preferred orientation aligned with the orientation of the regional $\sigma_{H\max}$. This is consistent with the presence of three different orientations of mafic dike swarms in the study area, each of which is different from the others and corresponds with the size of the islands in the study area. Fracture mechanics also suggest that the trachyte magma has more than double the magma overpressure p_{os} than the trachybasalt magma p_{om}. The magma overpressure and dike tip stress associated with silicic magmas are large enough to counteract the pressure, in which the dike follows to propagate in a preferred orientation governed by the 6.9–16 MPa regional stress field (see Section 2.4).

5.3. Implications for volcano-tectonic stress orientation

The present results suggest that the orientation of intrusions within the ODS reflects the relationship between dike tip pressure and magma overpressure and the surrounding regional stress field. Dike tip pressure and magma overpressure both positively correlate with the SiO_2 concentration in magma. Fracture mechanics suggests that these characteristics are determined by a balance between magma and host rock densities and magma chamber depth, all of which decrease with increasing SiO_2. The development of a dike swarm also requires similar processes to be repeated in such a way to form a regional-scale preferred orientation defined by the intrusion of multiple dikes.

The preferred orientation of dikes and sills within the ODS correlates with magma composition, as reflected by SiO_2 concentrations. This clear difference in preferred orientation represents a difference in magma overpressure between the mafic and silicic magmas. This in turn means that a comparative analysis of stress fields at different scales could provide insights into the orientation of volcano-tectonic stress in an area, indicating that dike orientations may not fully reflect the tectonic stress field of an area during emplacement.

6. Conclusions

A detailed field, geochronological, and geochemical study of the Late Miocene Oki-dozen dike swarm (ODS) of southwest Japan provided the following insights into the effects of the regional stress field on volcano-tectonic orientations.

Swarms of parallel trachybasalt and trachyandesite dikes in the study area can be grouped by orientation to NW-SE, N-S, and NE-SW sets. In addition, more evolved trachytic magmas form dikes and sills that radiate from the central Oki-dozen volcanic complex, suggesting that these more silicic magmas were emplaced when the magnitude of horizontal stress was similar in all directions.

The maximum thickness of 37 dikes was compared with their SiO_2 concentrations, yielding a critical thickness (T_{cr}) relationship that can be approximately expressed as $T_{cr} = 0.2 \times (SiO_2 - 40)$. Our data suggest that the orientation of intrusions within the ODS is a function of dike tip pressure and magma overpressure, both of which vary with SiO_2 concentration. These characteristics are in turn determined by magma and host rock densities and the depth of the parental magma chamber.

The preferred orientation of dikes and sills within the ODS is related to the SiO_2 content of the magma, with mafic magmas being intruded along three locally parallel preferential orientations, whereas the silicic dikes and sills form a radial arrangement. This clear difference in preferred orientation is the result of differences in magma overpressure between the mafic and silicic magmas, where the estimated magma overpressure of ~15 MPa and the dike tip pressure of ~60 MPa within the silicic magmas were large enough to counteract the effects of the 6.9–16 MPa regional stress. In contrast, the mafic dike swarm is aligned as a result of the effect of the regional stress field, albeit with small amounts of differential stress. The development

of a regional-scale dike swarm requires these processes to be repeated to ensure the dikes of the swarm have a common orientation. As such, the comparative analysis of different scales of stress fields would provide significant insights into the orientation of regional volcano-tectonic stress.

Acknowledgements

We thank Prof. Y. Itoh for providing the opportunity to undertake this research and for encouragement in preparing the manuscript. DM, KT, KA, and TW also thank T. Chiba for assistance during fieldwork.

Author details

Daisuke Miura[1]*, Kiyoshi Toshida[1], Ken-ichi Arai[2], Takeshi Wachi[2†] and Yutaka Wada[3]

*Address all correspondence to: dmiura@criepi.denken.or.jp

1 Geosphere Sciences, Central Research Institute of Electric Power Industry, Abiko, Japan

2 Asia Air Survey, Kawasaki, Japan

3 Nara University of Education, Nara, Japan

† Present address: In Situ Solutions, Tokyo, Japan

References

[1] Rubin AM. Propagation of magma-filled cracks. Annual Review of Earth and Planetary sciences. 1995;23:287-336. doi:10.1146/annurev.ea.23.050195.001443

[2] Gudmundsson A. Rock fractures in geological processes: Cambridge University Press. Cambridge, UK. 2011. 578 p. doi:10.1017/CBO9780511975684

[3] Takada A. The influence of regional stress and magmatic input on styles of monogenetic and polygenetic volcanism. Journal of Geophysical Research. 1994;99:13563-13573. doi:10.1029/94JB00494

[4] Seaman SJ, Scherer EE, Standish J. Multistage magma mingling and the origin of flow banding in the Aliso lava dome, Tumacacori Mountains, southern Arizona. Journal of Geophysical Research. 1995;100:8381-8398. doi:10.1029/94JB03260

[5] Tuffen H, Dingwell D: Fault textures in volcanic conduits: evidence for seismic trigger mechanisms during silicic eruptions. Bulletin of Volcanology. 2005;67:370-387. doi:10.1007/s00445-004-0383-5

[6] Pallister JS, Cashman KV, Hagstrum JT, Beeler NM, Moran SC, Denlinger RP. Faulting within the Mount St. Helens conduit and implications for volcanic earthquakes. Geological Society of America Bulletin. 2013;125:359-376. doi:10.1130/B30716.1

[7] Cashman KV, Sparks RSJ. How volcanoes work: A 25 year perspective. Geological Society of America Bulletin. 2013;125:664-690. doi:10.1130/B30720.1

[8] Cruden AR. Flow and fabric development during the diacritic rise of magma. Journal of Geology. 1990;98:681-698. doi:10.1086/629433

[9] Webb SL, Dingwell DB. Non-Newtonian rheology of igneous melts at high stresses and strain rates: Experimental results for rhyolite, andesite, basalt, and nephelinite. Journal of Geophysical Research. 1990;95:15695-15701. doi:10.1029/JB095iB10p15695

[10] Cashman K, Blundy J. Degassing and crystallization of ascending andesite and dacite. Philosophical Transactions of the Royal Society of London A, Mathematical, Physical, and Engineering sciences. 2000;358:1487-1513. doi:10.1098/rsta.2000.0600

[11] Blundy J, Cashman K. Ascent-driven crystallisation of dacite magmas at Mount St Helens, 1980-1986. Contributions to Mineralogy and Petrology. 2001;140:631-650. doi:10.1007/s004100000219

[12] Takeuchi S. Preeruptive magma viscosity: An important measure of magma eruptibility. Journal of Geophysical Research. 2011;106:B10201. doi:10.1029/2011JB008243

[13] Marsh BD. On the crystallinity, probability of occurrence, and rheology of lava and magma. Contributions to Mineralogy and Petrology. 1981;78:85-98. doi:10.1007/BF00371146

[14] Scaillet B, Holtz F, Pichavant M. Phase equilibrium constraints on the viscosity of silicic magmas. 1. Volcanic-plutonic comparison. Journal of Geophysical Research. 1998;103: 27257-27266. doi:10.1029/98JB02469

[15] Brenna M, Nakada S, Miura D, Toshida K, Ito H, Hokanishi N, Nakai S. A trachyte–syenite core within a basaltic nest: filtering of primitive injections by a multi-stage magma plumbing system (Oki-Dozen, south-west Japan). Contributions to Mineralogy and Petrology. 2015;170:22. doi:10.1007/s00410-015-1181-0

[16] Toshida K, Miura D, Hataya R. Proposition of assessment method for lateral magma migration – Effects of magma geochemistry studied from the distribution of conduits at Oki Dozen volcano– (in Japanese with English abstract). CRIEPI Report. 2006; N05026;24 p.

[17] Morris PA, Itaya T, Iizumi S, Kagami H, Watling RJ, Murakami H. Age relations and petrology of alkalic igneous rocks from Oki Dozen, Southwest Japan. Geochemical Journal. 1997;31:135-154. doi:10.2343/geochemj.31.135

[18] Tiba T, Kaneko N, Kano K. Geology of the Urago District—with 1:50,000 geological sheet map (in Japanese with English abstract). Geological Survey of Japan; 2000. 74 p.

[19] Kaneko N, Tiba T. Occurrence and K–Ar age of an alkali olivine basalt from Nakanoshima in Oki-Dozen, Shimane Prefecture, Southwest Japan (in Japanese with English abstract). The Journal of the Geological Society of Japan. 1998;104:419-422. doi:10.5575/geosoc.104.419

[20] Wada Y, Itaya T, Ui T. K–Ar ages of Oki-Dozen and Tango dike Swarms, Western Honshu, Japan (in Japanese with English abstract). Bulletin of Volcanological Society of Japan. 1990;35:217-229.

[21] Kano K, Kaneko N, Ishizuka O, Tiba T, Yanagisawa Y. The beginning and lifetime of Dozen volcano, Oki Islands, SW Japan (in Japanese with English abstract). Bulletin of the Volcanological Society of Japan. 2014;59:77-88.

[22] Itoh Y, Nakajima T, Takemura A. Neogene deformation of the back-arc shelf of Southwest Japan and its impact on the palaeoenvironments of the Japan Sea. Tectonophysics. 1997;281:71-82. doi:10.1016/S0040-1951(97)00159-5

[23] Nakamura K. Volcanoes as possible indicators of tectonic stress orientation—principle and proposal. Journal of Volcanology and Geothermal Research. 1977;2:1-16. doi:10.1016/0377-0273(77)90012-9

[24] Mogi K. Relations between the eruptions of various volcanoes and the deformations of the ground surfaces around them. Bulletin of the Earthquake Research Institute, University of Tokyo. 1958;36:99-134.

[25] Nakata E. The proposal of chemical analysis method of sedimentary rocks by X ray fluorescence – The combination analysis of pressed powder method and glass bead method (in Japanese with English abstract). CRIEPI Report. 2006;N05063;24 p.

[26] Le Bas MJ, Le Maitre RW, Streckeisen A, Zanettin BA. Chemical classification of volcanic rocks based on the total alkali–silica diagram. Journal of Petrology. 1986;27:745-750. doi:10.1093/petrology/27.3.745

[27] Pinkerton H, Steavenson RJ. Methods of determining the rheological properties of magmas at sub-liquidus temperatures. Journal of Volcanology and Geothermal Research. 1992;53:47-66. doi:10.1016/0377-0273(92)90073-M

[28] Taniguchi H. On the volume dependence of viscosity of some magmatic silicate melts. Mineralogy and Petrology. 1993;49:13-25. doi:10.1007/BF01162923

[29] Wada Y. On the relationship between dyke width and magma viscosity. Journal of Geophysical Research. 1994;99:17743-17755. doi:10.1029/94JB00929

[30] Geshi N, Kusumoto S, Gudmundsson A. Geometric difference between non-feeders and feeder dykes. Geology. 2010;38:195-198. doi:10.1130/G30350.1

[31] Browning J, Drymoni K, Gudmundsson A. Forecasting magma-chamber rupture at Santorini volcano, Greece. Scientific Reports. 2015;5:15785. doi:10.1038/srep15785.

INTECH